The Mössbauer Effect

PHYS352 Experimental Modern Physics
William&Mary

March 2022

1 Introduction

In 1957 Rudolf Mössbauer discovered the effect which bears his name almost accidentally [1]. He was studying resonance fluorescence – the process in which γ-rays are resonantly scattered from nuclei – as a function of temperature. At low temperature this process was expected to turn off because the recoils given to the emitting nucleus and to the absorbing nucleus would cause the emitted γ-ray to not be at the right energy to resonantly interact with the absorbing nucleus (more about it later). Mössbauer, however, observed an increase in scattering rather than the expected decrease at low temperature. The explanation of this surprising effect brought him a Nobel prize, created a new approach for precision nuclear spectroscopy, and became a popular tool for generations of physicists and chemists.

So let's first understand why Mössbauer finding was so counter-intuitive. To do that, we need to examine a little more closely the process of resonant fluorescence: a process in which a system transitions from excited to ground state by emitting a quanta of radiation at the energy matching the energy difference between these two states. This process is what responsible for, e.g., fluorescent lights, in which electrons, excited by the discharge, emit visible light as they cascade down the atomic energy levels to the ground state. Similar process is possible for nuclei, albeit at much higher energies. This lab uses ^{57}Fe, which is the most common Mösbauer element nowadays. The pertinent information for ^{57}Fe are shown in Table **??**. (Just as a note, originally Mössbauer studied ^{191}Ir, a much more difficult nucleus to study.) Fig.1 shows how excited iron nuclei are created through the decay of the radioactive^{57}Co, emitting a γ-quanta at $E_0 = 14.4$ kEv as excited ^{57}Fe return to the ground state. When emitted, however, the 14.4 keV γ-ray gives a recoil momentum, to the emitting nucleus $P_r = E/c$ (thanks to the momentum conservation). This corresponds to the recoil energy:

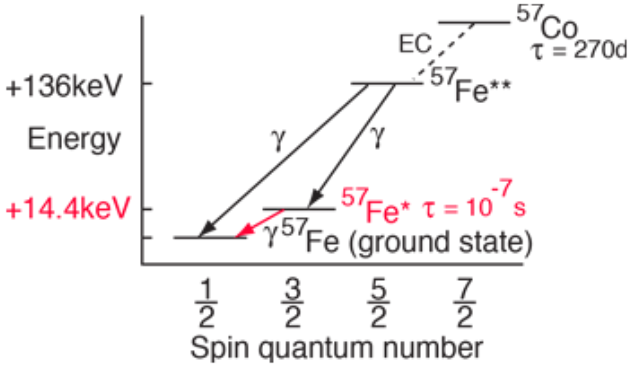

Figure 1: Radioactive decay of ^{57}Co $\rightarrow^{57}$ Fe*, resulting in emission of 14.4keV γ-rays [**?**]

.

$$E_r = P_r^2/(2M_{Fe}) = .018 \text{ eV}, \tag{1}$$

where M_{Fe} is the mass of a single Fe nucleus. Thus, to conserve the energy, the actual energy of the emitted γ-quanta must be lower that exact transition energy E_0 by the recoil amount: $E_0 - E_R$. Similarly,

a nucleus absorbing a γ-quanta experiences a similar recoil. Thus, in order to enable the absorption, a γ-quanta must carry enough energy $E_0 + E_R$ to excite the nucleus to the excited state *and* provide sufficient energy for recoil, it

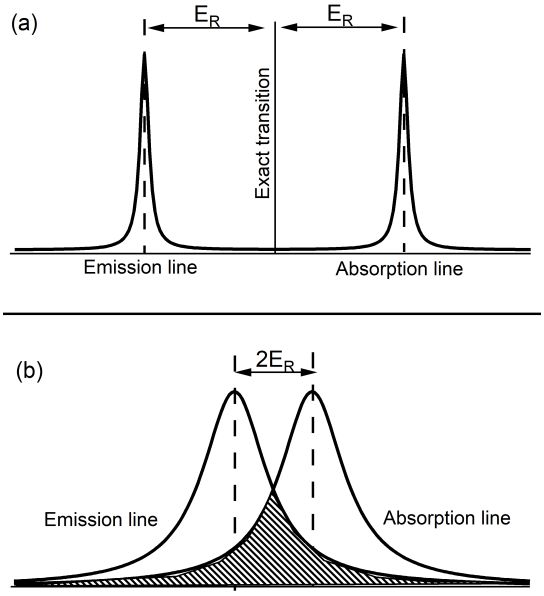

Figure 2: Diagram showing the energy shift of an emitted or absorbed γ-ray due to the recoil of the nucleus. (a) The recoil is much larger than a resonance linewidth $E_R \gg \Gamma$ (the situation expected for a single-nucleus recoil at low temperatures), and thus the reabsorption is impossible. (b) the case of the recoil energy comparable with the linewidth $E_R \simeq \Gamma$. In this case the overlap area is relatively large, and roughly corresponds to the re-absorption probability.

So is it possible for a nucleus to reabsorb what was emitted by another nucleus? To answer that question we must consider the spectral width of the emission and absorbing lines. At low temperatures and clean materials this linewidth is determined by the finite lifetime of the excited state because of the uncertainty principle:

$$\Gamma = \hbar/\tau = 4.7 \times 10^{-9}\ \text{eV},$$

which is significantly smaller than the expected recoil energy. This situation is illustrated in Fig. 2, that shows that under normal circumstances the energy of the emitted photon will be too low to be reabsorbed by similar nuclei. So at low temperature the emission and absorption lines will not overlap and so resonant scattering should not occur. At higher temperature the resonance tends to broaden, increasing the overlap between the resonances, as shown in Fig. 2(b).

So how could Mössbauer possibly observe an *increase* in scattering and absorption of the emitted γ rays when he cooled his samples, rather than the expected decrease? The explanation is that for some of the γ-rays the recoil momentum is given not to individual emitting or absorbing nuclei, but is shared with the whole crystal lattice in which these nuclei are embedded. In this case the mass M_{Fe} in Eq. 1 is multiplied by the number of atoms in the sample (that is on the order of Avogadro's number), making the recoil energy immeasurably small. Here we are not going to discuss why this happens, but a good undergraduate-level tutorial can be found here [3, 4]. However, since in this case the recoil energy is effectively zero, there is an almost complete overall between the absorption and emission line in Fig. 2(b). Since the linewidth is still very narrow, we are now able to observe a very narrow but strong absorption line. In this lab we are going to take advantage of it to probe the internal energy level structure of the iron nuclei in different environments.

What makes Mössbauer spectroscopy such a useful tool is that it helps uncover the energy level structure of nuclei with high precision, thanks to its extremely narrow spectral linewidth. As we just discussed, in order for the emitter's radiation to be absorbed by the target, the source energy must match the energy difference between two states in the absorber, i.e., be on resonance. So to experimentally observe the nuclear transitions and measure their shifts, we must controllably change the source energy and measure the positions of the absorption lines, thus experimentally measuring the energies of various transitions in the target nuclei. In case of the Mössbauer apparatus such tuning is provided by linear Doppler effect: the

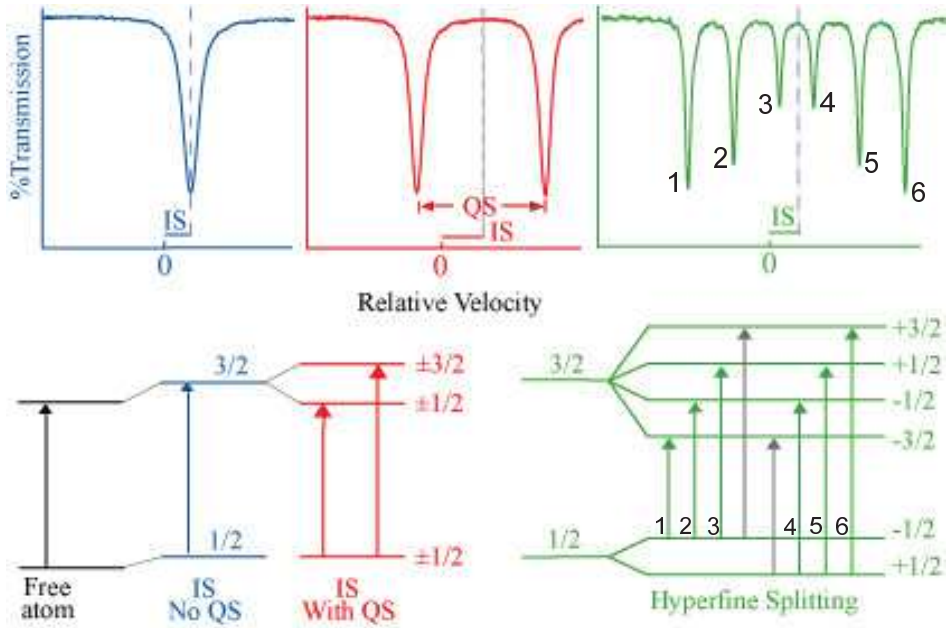

Figure 3: Absorption spectra for various characteristic shifts and splittings. Blue: isomer shift; red: isomer shift + quadrupoe splitting; green: isomer shift + magnetic hyperfine splitting

energy of radiation, emitted by a moving source is shifted by ΔE:

$$\frac{\Delta E}{E_0} = \frac{v}{c}, \tag{2}$$

where v is the velocity of the moving source and c is the speed of light.

2 Nuclear Energy Level Structure

While the basic energy levels of a nuclei, just like of an atom, are defined by the internal forces keeping them together, its surroundings can affect it, resulting in relatively small changes in each level energy. Such perturbation usually manifest themselves as various energy shifts and level splittings. When measured, these variations provide priceless information about internal structure of materials, and are widely used for chemical analysis of various crystals and alloys. In The most common interactions affecting the nuclear structure are *the isomer shift*, the *nuclear quadrupole splitting* and the *nuclear magnetic dipole splitting*. These effects are shown schematically in Fig. 3. All these shifts are caused by interaction of nuclei with nearby electrons, and are often characterized as *hyperfine* interactions.

2.1 Isomer Shift

The isomer shift, sometimes known as the chemical shift, originates from interactions of nuclear charge with the electron charge distribution within the nucleus. Only electrons in s orbital have non-zero probability are responsible, since only they have non-zero charge distribution at $r = 0$, although other electrons

may have some indirect effect through their influence on the s electrons.

$$E_a - E_e = \frac{2}{5}\pi Z e^2 [R_{is}^2 - R_{gr}^2][|\psi(0)_a|^2 - |\psi(0)_e|^2] \tag{3}$$

Here, $R_{is/gr}$ are the radii of the isomeric state and ground state respectively and $|\psi(0)_{a/e}|^2$ are the electron densities at the nucleus for the absorbing and emitting atoms [2]. For pure Fe^{57} the isotopic shift is set to zero by definition. Since the isomer shift measures the charge density of the atomic electrons at the nucleus, it is often used in chemistry to study chemical bonding and covalency.

2.2 Quadrupole Splitting

Quadrupole splitting of nuclear energy levels exists for nuclei in states with non-spherical charge distributions (those with spin quantum number I greater than 1/2) that may have a nuclear quadrupole moment Q. In this case the surrounding electric field gradient V_{zz} splits the nuclear energy levels with different values of the magnetic quantum number $|m|$. A simplified expression, assuming the electric field gradient only in z-direction can be written as:

$$E_{QS} = eQV_{zz}\frac{3m^2 - I(I+1)}{4I(2I-1)} \tag{4}$$

where the quadrupole moment $Q = \frac{1}{e}\int \rho(3z^2 - r^2)d^3r$, with ρ being the nuclear charge density.

In case of iron nuclei, the excited state $I = 3/2$ splits into two, with slightly different energies for $m = \pm 1/2$ and $m = \pm 3/2$, as shown in Fig. 3.

2.3 Zeeman Splitting

The Zeeman splitting (also known as magnetic hyperfine splitting) is caused by the interaction of the nuclear magnetic moment μ with any surrounding magnetic field $\mathbf{H}$. The energy sublevels with different azimuthal quantum numbers m are shifted by different amount $E_{I,m}$:

$$E_{I,m} = -\boldsymbol{\mu} \cdot \mathbf{H} = -g_I \mu_{nm} m H \tag{5}$$

Here g_I is the Landé g-factor – a dimensionless parameter that characterizes the nuclear magnetic moment of state I in the units of *nuclear magneton* $\mu_{nm} = 3.15 \cdot 10^{-8}$ eV/T, m is the magnetic quantum number, and H is the magnetic field (in Tesla). While both internal (produced by nearby electrons) and external fields can contribute into H, the internal contribution typically dominates (compare $\approx$ 330 kG for the internal magnetic field in pure iron with 0.5G Earth magnetic field).

Fig. 3 shows that the ground state with $I = 1/2$ splits into two states, corresponding to $m = \pm 1/2$, and the excited state with $I = 3/2$ splits into two states, corresponding to $m = \pm 1/2, \pm 3/2$. However, since the photon angular momentum is 1, only transitions with $\Delta m = 0, \pm 1$ are possible. Thus, there are six possible (allowed) transitions, shown in green arrows in Fig. 3; the two black arrows indicate the forbidden (impossible) transitions.

To calculate the energy of each transition, one needs to find the energy difference between the particular ground and excited Zeeman states. For example, the transition requiring the minimum amount of energy occurs (labeled "1" in Fig. 3) occurs between the ground $I = 1/2; m = -1/2$ state (energy $E_{1/2;-1/2} = 1/2 g_{1/2}\mu_{nm}H$) and excited $I = 3/2; m = -3/2$ state (energy $E_{2/2;-3/2} = E_e - 3/2 g_{3/2}\mu_{nm}H$). The corresponding transition energy E_1 is then

$$E_1 = E_e - 3/2 g_{3/2}\mu_{nm}H - E_{1/2;-1/2} = E_0 - 1/2(3g_{3/2} + g_{1/2})\mu_{nm}H. \tag{6}$$

To find the energy splitting between different peaks in a Mössbauer spectrum one needs to difference between two transitions. For example, the splitting between the two neighbouring peaks "2" and "1" is

$$E_2 - E_1 = [E_0 - 1/2(g_{3/2} + g_{1/2})\mu_{nm}H] - [E_0 - 1/2(3g_{3/2} + g_{1/2})\mu_{nm}H] = g_{3/2}\mu_{nm}H. \quad (7)$$

Note that this difference is equal to the energy splitting between two closest excited Zeeman states, since both transition originate from the common ground state. To determine the energy splitting between the two ground states we need to measure the separation between the transitions "2" and "4" (or "3" and "5"), that originate from two different ground states, but have a common excited state.

$$E_4 - E_2 = [E_0 - 1/2(g_{3/2} - g_{1/2})\mu_{nm}H] - [E_0 - 1/2(g_{3/2} + g_{1/2})\mu_{nm}H] = g_{1/2}\mu_{nm}H. \quad (8)$$

2.4 Resonance linewidth

According to the uncertainty principle, any excited state with finite lifetime must have a minimum spectral width of $\Gamma_a = \hbar/\tau$. The 14.4 keV excited state has the average lifetime $\tau = 141.8(5)$ns and the corresponding $\Gamma_a = 4.67 \cdot 10^{-9}$ eV. Note that this width is more than 10^9 times narrower than the energy of the γ quanta, making this one of the most accurate spectral probes! For that reason the Mössbauer spectroscopy was used for the first experimental demonstration of the gravitational red shift [5].

It is very convenient to use the value of *absorption cross-section* σ_E – the absorption coefficient per each atom – to characterize the relative amount of the radiation absorbed at the target. of the radiation as a function of the radiation energy. If the spectral widths of emitter and absorber are similar and, for example, determined by the finite lifetime of the excited state $\Gamma_a = \hbar/\tau$, then it is possible to calculate the expression for the resonance absorption cross-section:

$$\sigma(E) = \sigma_0 \frac{(\Gamma_a/2)^2}{(E - E_0)^2 + (\Gamma_a/2)^2}, \quad (9)$$

where E_0 is the exact resonance energy, E is the energy of the γ radiation, and $\sigma_0 = 1.5 \cdot 10^{-18}$ cm^2 is the resonant Mössbauer absorption cross-section.

In some materials, however, the absorption resonance can be broadened. For example, in stainless steel sample we expect the measured resonance linewidth Γ_a can be broader than $\hbar/\tau$. This is the case of the inhomogeneous broadening - in plain language that means that each nucleus finds itself in slightly different environment due to random interactions with other neighbours. As a result, each nucleus energy levels experiences a small random shift. As a result, the range of energies in which absorption takes place becomes larger than expected. In this case the resonance is said to be "broadened".

	Ground state	First Excited state
Energy E_0 (keV)	0	14.4
Isospin I	1/2	3/2
g-factor g_I	0.1812	−0.102
Quadrupole moment Q (barns)	0	0.21(2)
Mean liftime τ (s)	stable	$1.41 \cdot 10^{-7}$

Table 1: Useful ^{57}Fe Properties.

3 Apparatus

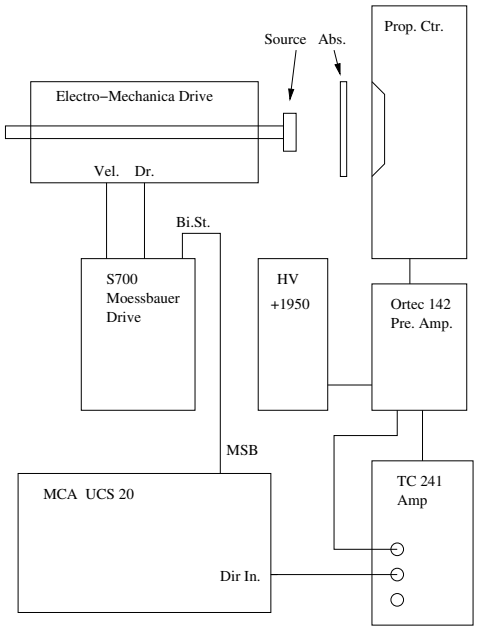

Figure 4: Block diagram of the Mössbauer apparatus.

A block diagram of the apparatus is shown in Fig. 4. A ^{57}Co source is attached to the rod of the electromechanical drive, that can move back and force with constant acceleration (i.e., with linear change in its velocity). Following electron capture and transition to the 14.4 keV, $I = 3/2$ excited nuclear state, a γ-ray is emitted. The γ-ray traverses an absorber, and those that are not absorbed proceed to a proportional counter. This proportional counter has a thin Be window to allow the γ-ray through, is filled with a special gas, and has a small diameter central wire at high voltage (around 2000V). The entering γ-ray causes an atom to eject an electron with nearly the full γ-ray energy. This electron ionized further atoms. The electrons drift toward the central electrode and are accelerated to produce proportionally more electrons (hence the name). The charge is passed to an amplifier that produces a voltage pulse proportional to the charge and, correspondingly, to the γ-ray energy. This pulse is sent to a computer controlled multi-channel analyzer (MCA) which makes a histogram of pulse heights. Please follow the instructions in the manufacturer's manual to start the experiment and obtain the Mössbauer spectra.

4 Measurements

During this lab, you will obtain the Mössbauer spectra for several samples.

Enriched ^{57}Fe This is a ferromagnetic and has a large internal magnetic field. This element is normally used for calibration, as its isometic shift is zero, its crystal structure exhibits no quadrupole splitting. Since its internal magnetic field is well-known, you will be able to use it to calibrate the channel velocities.

Na-Prusside Non-magnetic alloy that exhibits quite strong quadrupole splitting.

Stainless Steel This is a non-magnentic alloy of iron, and thus produces a single absorption line. However, some local inhomogeneities may broaden this resonance.

Magnetite This ferric oxide (Fe_3O_4) has one of the strongest internal magetic fields, and thus exhibits the magnetic hyperfine splitting significantly larger than theat of metallic iron. Moreover, in magnetite iron atoms can occupy two different sites inside the crystal lattice, experiencing two slightly different values of the internal magnetic field.

The samples of data for each samples are shown in Fig. 5.

4.1 Calibration

Use the known splittings (shown in Table 2) between the six resonances of the enriched ^{57}Fe to calibrate the velocity scale of the mechanical drive.

m_g	m_e	Shift (mm/s)
-1/2	-3/2	-5.328
-1/2	-1/2	-3.084
-1/2	+1/2	-0.840
+1/2	-1/2	+0.840
+1/2	+1/2	+3.084
+1/2	+3/2	+5.328

Table 2: Zeeman shifts of the ^{57}Fe nuclei .

4.2 Zeeman Field

Determine the magnetic field at the ^{57}Fe in iron for both the ground and excited states. Compare this value with 330 kG (or 33 T).

4.3 Quadrupole Slitting

Using the calibration, determine the energy splitting between the two excited states in Na-Prusside. Using the known value of the quadrupole moment of the excited state Q, determine the electric field gradient V_{zz}. Estimate the distance from an electronic charge which would give this electric field gradient.

4.4 Resonance linewidth and the effect of the impurities

Fit one of the Na-Prusside absorption lines to Lorentzian line shape:

$$d(v) = A - \frac{B}{(v - C)^2 + (D/2)^2}, \tag{10}$$

where $d(v)$ is the count distribution for different velocities v. Comparing the fit function with Eq. 9, identify the physical meaning for each of the fitting parameters A, B, C and D. Using the calibration, determine $\Gamma_e xpt$ and compare it with the expected value for the life-time limited excited state linewidth.

Repeat the fitting procedure for the stainless steel sample. Try to explain why in this case the resonance linewidth is noticeably broader.

4.5 Chemical composition analysis

Mössbauer spectra are widely used to determine the local environment of Fe nuclei inside various compounds. For example, the Mössbauer spectrum for the magnetite Fe_3O_4 consists of two six-line patterns with relatively narrow lines and can be accurately fitted with two sextets. The outer sextet is attributed to Fe3+ on A-sites of magnetite, while the inner sextet is attributed to iron atoms located on B-sites of spinel structure. The difference in the Zeeman splittings for each site is determined by the difference in the local magnetic field values for two possible iron locations. Using the procedure above, estimate the magnetic field values for both A- and B-sites in magnetite.

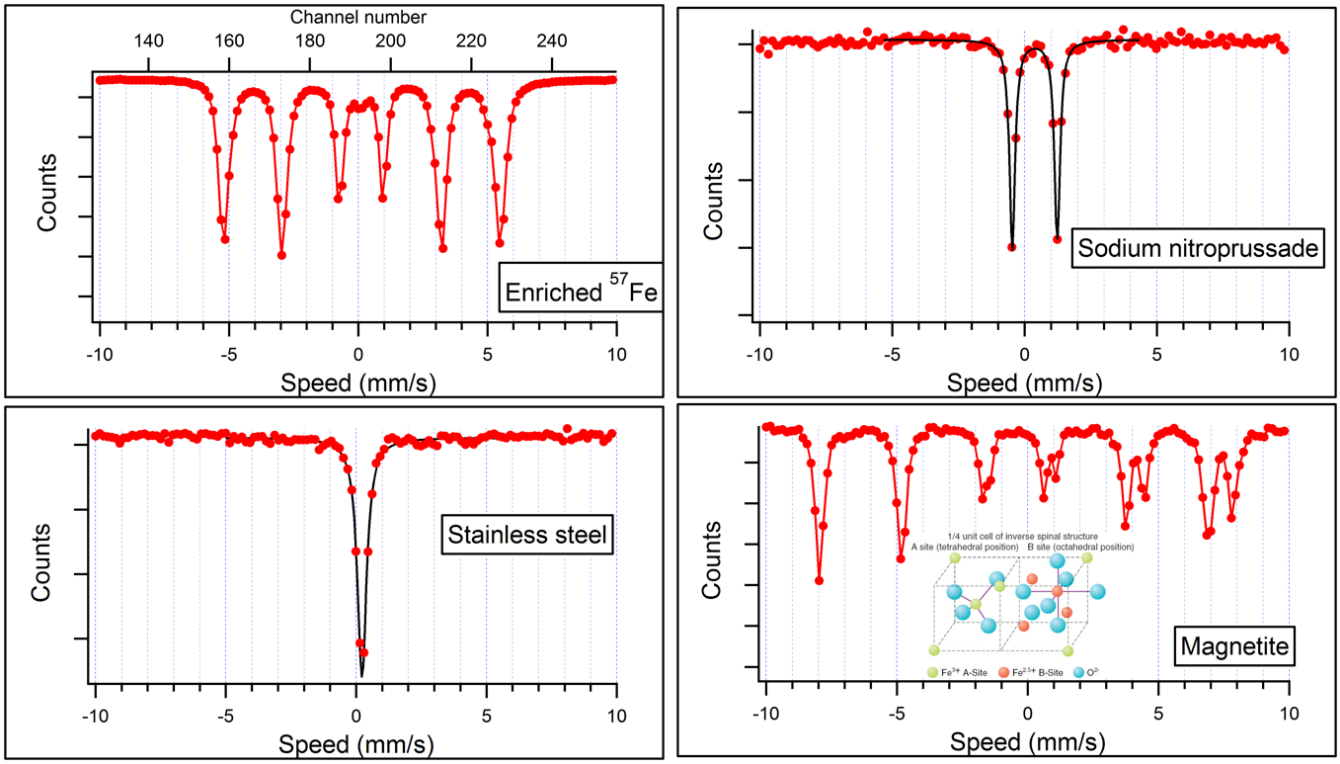

Figure 5: Examples of expected experimental Mössbauer specra for different materials. When shown, black lines represent the fit of the data with Lorentzian function (Eq. 10) or with the sum of two Lorentzian functions of equal width. For the magnetite, the schematic of the crystal structure is shown, indicating two possible placements for Iron.

References

[1] R.L. Mössbauer, "Kernresonanzfluoreszenz von Gammastrahlung in Ir191", *Z. Physik* **151**, 124–143 (1958).

[2] Gunther K. Wertheim (1964) *Mössbauer Effect: Principles and Applications*, Academic Press.

[3] Leonard Eyges, "Physics of the Mössbauer Effect," *Am. J. Phys.* **33**, 790 (1965); doi: 10.1119/1.1970986

[4] Principi, G. "The Mössbauer Effect: A Romantic Scientific Page," *Metals* **10**, 992 (2020); https://doi.org/10.3390/met10080992

[5] Cranshaw, T.E.; Schiffer, J.P.; Whitehead, A.B. "Measurement of the gravitational red shift using the Mössbauer effect in Fe57," *Phys. Rev. Lett.* **4**, 163–164 (1960).

[6] M. Seto et al., "Site-Specific Phonon Density of States Discerned Using Electronic States," *Phys. Rev. Lett.* **91**(18), 185505 (2003).